Exceptional points in a dielectric spheroid

Evgeny Bulgakov,[1,2] Konstantin Pichugin,[1] and Almas Sadreev ⬤[1]

[1]*Kirensky Institute of Physics, Federal Research Center KSC SB RAS, 660036 Krasnoyarsk, Russia*
[2]*Reshetnev Siberian State University of Science and Technology, 660037 Krasnoyarsk, Russia*

Evolution of resonant frequencies and resonant modes as dependent on the aspect ratio is considered in a dielectric high index spheroid. Because of rotational symmetry of the spheroid the solutions are separated by the azimuthal index *m*. By the two-parametric variation of a refractive index and the aspect ratio we achieve exceptional points at which the resonant frequencies and resonant modes are coalesced in the sector $m = 0$.

I. INTRODUCTION

Optical properties of a dielectric particle are described by resonant frequencies and corresponding resonant modes. The most famous case is a dielectric sphere whose resonant modes and frequencies were first considered by Stratton [1]. The solutions in the form of quasinormal modes (QNMs) leaking from the sphere were considered in Refs. [2,3]. The frequencies of these solutions' resonances are complex because of coupling of the dielectric particle with the radiation continuum and can be considered as the eigenvalues of the non-Hermitian Hamiltonian [4–7]. Non-Hermitian phenomena drastically alters the behavior of a system compared to its Hermitian counterpart describing the closed system. The best example of such a difference is the avoided resonant crossing (ARC) when real or imaginary parts of complex eigenvalues of the non-Hermitian Hamiltonian undergo repulsion for variation of a parameter of the closed system [8–12]. In turn the ARC can emerge to singularities' exceptional points (EPs). In parameter-dependent eigenvalue problems of the non-Hermitian Hamiltonian, a special kind of degeneracy may occur at some particular values of the system parameters: two or more eigenvalues coalesce and their corresponding eigenfunctions collapse into one single function [13–15]. EPs are interesting because they give rise to unusual physical phenomena. Early experiments on microwave coupled resonators revealed the peculiar topology of eigenvalue surfaces near exceptional points for encircling of EP [16].

Many works on EPs and their applications are associated with parity-time (PT) symmetric optical systems with a balanced gain and loss. In that case, EPs can be easily found by tuning a single parameter, namely, the amplitude of the balanced gain and loss [17–21]. Since it is not always easy or desirable to keep a balanced gain and loss in an optical system it is of significant interest to explore EPs and their applications in non-PT-symmetric optical systems. Currently, there exist studies concerning EPs for resonant states in extended periodic dielectric structures sandwiched between two homogeneous half-spaces [22–25], dual-mode planar optical waveguides [26] and plasmonic waveguide [27], layered structures [28–30], two infinitely long dielectric cylinders [31–35], and even a single rod with deformed cross section [33,36–39]. As for compact dielectric resonators we distinguish the only study of EPs in a compact coated dielectric sphere [40].

In the present paper we consider a compact elementary dielectric resonator such as a spheroid in which EPs can be achieved by two-parametric variation of aspect ratio and refractive index. Although the spheroid allows the solution due to separation of variables in a spheroidal coordinate system [41,42], analytical expressions for solutions are too cumbersome. We use software package COMSOL MULTIPHYSICS, which allows one to obtain numerically the complex resonant frequencies and corresponding resonant modes of a particle of arbitrary shape embedded into the radiation continuum by use of perfectly absorbing boundary conditions.

II. EVOLUTION OF RESONANT FREQUENCIES IN A SPHEROID

In all realistic physical resonators there is a certain degree of dissipation of energy to the environment. This effect is responsible for a broadening of the peaks in the spectra and is typically quantified in terms of the so-called quality factor Q. These solutions, which have complex resonance frequencies, are known in the literature as resonant modes or morphology-dependent resonances [43], or quasinormal modes (QNMs) [4]. Computation of resonances of spherical particles from Lorenz and Mie is a trivial matter due to analytical theory [1]. The spheroid also has rotational symmetry that allows one to calculate the resonant frequencies and resonant eigenmodes separately for each azimuthal index *m* and calculate EM field configurations as series over the orbital momenta outside the spheroid [41]

$$\vec{E}^{(m)}(\vec{r}) = \sum_{l=1}^{\infty} \left[a_l^m \vec{M}_l^m(k\vec{r}) + b_l^m \vec{N}_l^m(k\vec{r}) \right], \quad (1)$$
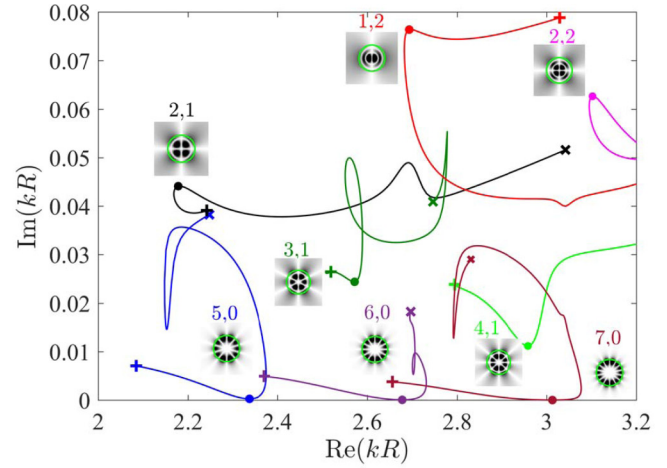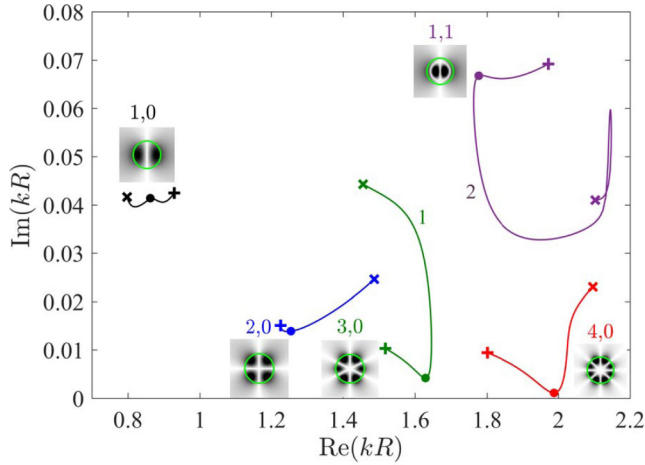
FIG. 1. Evolution of complex TE resonant frequencies in silicon spheroid with permittivity $\epsilon = 12$ for variation of aspect ratio of polar R_z and equatorial $R_\perp$ radii in the sector $m = 0$. Wave patterns show azimuthal component of electric field $|E_\phi|$ of the Mie resonant modes in sphere at points marked by closed circles where integers above the insets notify the orbital momentum l and the radial index n. "×" marks the case of oblate spheroid with $R_z = 0.4R_\perp$ while "+" marks the case of prolate spheroid with $R_z = 1.6R_\perp$.

where $\vec{M}_l^m$ and $\vec{N}_l^m = \frac{1}{k}\vec{\nabla} \times \vec{M}_l^m$ are the vector spherical harmonics [1,44] and k is the frequency. In what follows we consider the sectors $m = 0$ and $m = 1$.

The sector $m = 0$ is simplified compared to the sector $m = 1$ because of the separation of TE and TM modes. Figure 1 presents the evolution of complex TE resonant frequencies with variation of the equatorial radius $R_\perp$ relative to the polar radius R_z from oblate silicon spheroid $R_z = 0.4R_\perp$ to prolate spheroid $R_z = 1.6R_\perp$. k is the wave number and $R = (R_z R_\perp^2)^{1/3}$ is the mean radius that equalizes volumes of sphere and spheroid. For the reader's convenience we split the frequency range in Fig. 1 into two parts. The insets show the QNMs of a sphere. In Fig. 2 we demonstrate a phenomenon of avoided crossing of resonances marked as 1 and 2 in Fig. 1, which is the result of interaction of the dipole QNM with the octuple QNM [45]. There is a general belief that a homogeneous spherical dielectric body represents the ideal case, so that any perturbation of shape of the sphere can only degrade the resonance (the imaginary part increases or the Q factor decreases). Lai *et al.* [45,46] have shown this, however, provided that the imaginary part of the spherical QNM is small enough. For the QNMs with low Q factor their

frequencies deviate from the complex eigenfrequencies of the sphere linearly [4].

This anomalous behavior of the low-Q resonances can be comprehended if one refers to the series over spherical harmonics (1). For the TE polarization we have

$$\vec{E} = \sum_l a_l^0 \vec{M}_l^0, \tag{2}$$

where $l = 1, 3, 5, \ldots$ if the azimuthal component of electric field E_ϕ is even relative to $z \to -z$ and $l = 2, 4, 6, \ldots$ if E_ϕ is odd. Once a sphere transforms into a spheroid the orbital momentum l is not preserved. Figure 3 shows new multipole radiation channels are opened with this transformation. Let us consider some of the resonances shown in Fig. 1. For variation of the polar radius R_z the lowest mode shown by black line goes through the Mie dipole mode 1,0 of a sphere with the frequency $kR = 0.862 + 0.0414i$. As seen from the first subplot
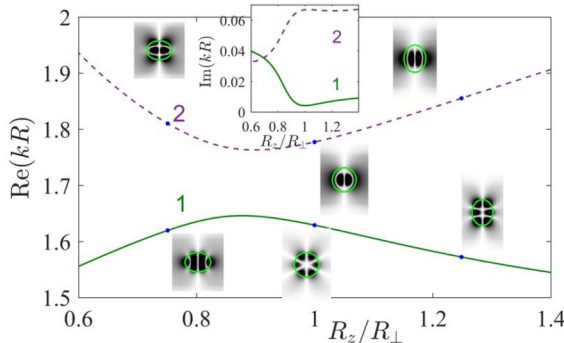

FIG. 2. Evolution of resonant frequencies and resonant modes labeled as 1 and 2 in Fig. 1 versus ratio of radii R_z and $R_\perp$.
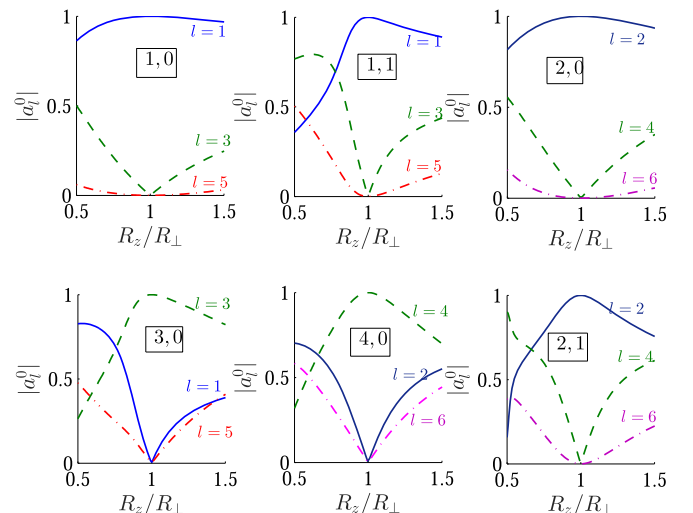

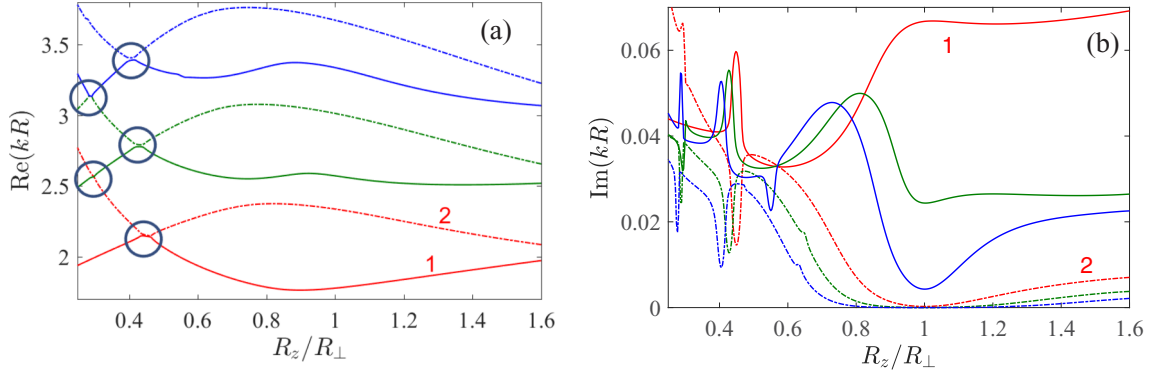FIG. 3. Evolution of multipole coefficients in series (1) for evolution of resonant modes l, n shown in Fig. 1.

FIG. 4. ARCs of TE QNMs for evolution of sphere into spheroid in the sector $m = 0$.

of Fig. 3 at this moment the only radiation channel is given by the coefficient a_{10}. The resonant widths of the Mie resonant modes fast fall down with the orbital momentum l and grow with the radial index n [47]. As a result, when a sphere is deformed, the fast decaying dipole channel is weakening at the cost of linear arising of the next slower decay octuple channel $l = 3$ in accordance to Eq. (2). These comprehensive considerations were issued by Lai *et al.* [45]. Respectively, the resonant width is decreased as shown in Fig. 1 by black line. However, there are exceptions from this rule, for example, the QNMs $l = 2, n = 1$ and $l = 2, n = 0$ (the last column of subplots in Fig. 3). In both cases the same slower decaying radiation channels with $l = 4$ and $l = 6$ are attaching to the quadruple channel with $l = 2$ for deviation from a sphere. Nevertheless the behavior of resonant widths is dramatically different as seen from Fig. 1. For the radial quantum $n = 0$ we observe a degradation of the quadruple QNM, while for $n = 1$ we observe the opposite behavior. That shows the importance of the radial indices for resonant widths [47].

Let us consider also the resonances evolving with the Mie resonances with higher orbital momentum, and octuple resonance 3,0 with the frequency $kR = 1.629 + 0.0042i$ shown by green line in Fig. 1. Corresponding evolution of multipole coefficients is shown in Fig. 3 in the subplot labeled 3,0. In contrast to previous dipole and quadruple resonances the

high-Q decaying octuple resonance is substituted by the fast decaying dipole resonance 1,0. As a result we observe an increase of resonant width in Fig. 1 for transformation of sphere into spheroid. The other subplot 4,0 in Fig. 3 shows the same result.

We omit analysis of the TM resonances because of a similarity with the case of the TE resonances. The reader can see the TM resonances in Ref. [48]. Also we present there the sector $m = 1$ destined to show that the phenomena of ARCs exist in the other sectors of the azimuthal index m, in particular, $m = 1$. Similar to the TE resonances in the sector $m = 0$ we observe the same tendency of degradation of the high-Q QNMs and, visa versa, enhancement of the Q factor for the low-Q QNMs for deformation of sphere [48].

III. EXCEPTIONAL POINTS

EPs arise in the vicinity of ARCs, numerous examples of which are shown in Fig. 4 highlighted by open circles. It is interesting that the ARC phenomena are observed only for the oblate spheroids below $R_z/R_\perp = 1/2$. Figure 5 demonstrates an exchange of the resonant modes typical for ARC for variation of the aspect ratio of spheroid. As shown in Fig. 4(b) the ARCs are complemented by strong enhancement of the
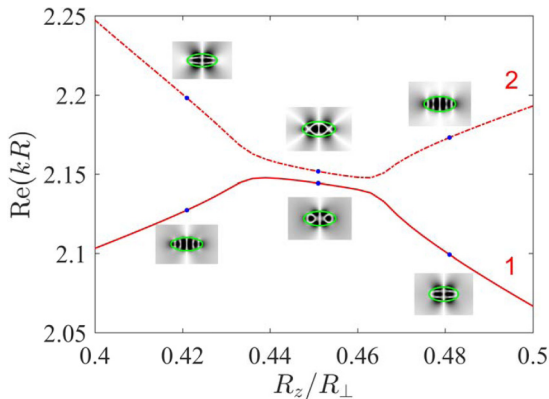

FIG. 5. Evolution of selected resonant frequencies and resonant modes labeled as 1 and 2 in Fig. 4 vs ratio of radii R_z and $R_\perp$. The insets show the azimuthal component $|E_\phi|$ of corresponding resonant modes at points marked by closed circles.
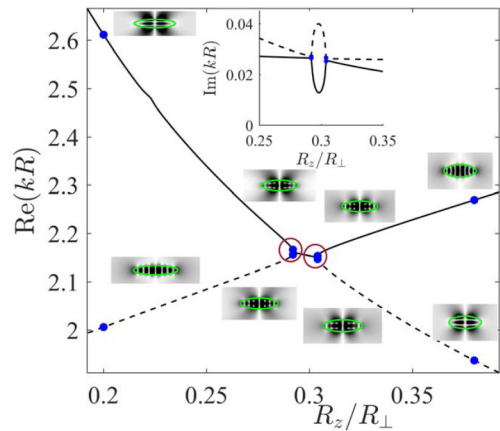

FIG. 6. Evolution of resonant frequencies and resonant modes versus $R_z/R_\perp$ at $\epsilon = 17.2$ in the sector $m = 0$. Open circles highlight EPs. The left one at $R_z/R_\perp = 0.292$, $\epsilon = 17.2$ and the right one at $R_z/R_\perp = 0.304$, $\epsilon = 18.4$. The insets show the $|E_\phi|$ profiles of TE QNMs at points marked by closed circles.
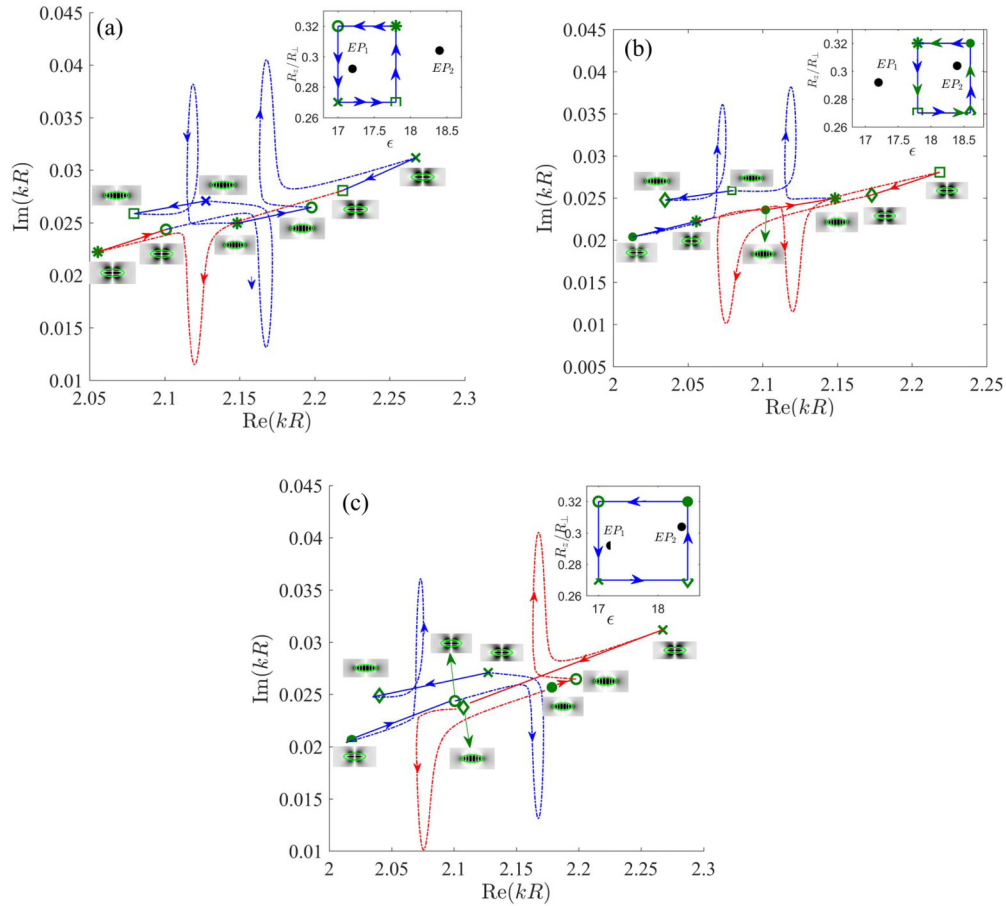
FIG. 7. Encircling of EPs shown by open circles in Fig. 6. (a),(b) Encircling separate EPs. (c) Encircling of both EPs. Insets show the component E_ϕ of resonant mode.

Q factor in an agreement with numerous considerations in different dielectric resonators [10,49–51]. Although the point $\epsilon = 17.2$ and $R_z/R_\perp = 0.45$ is not the exact EP point, one can see from Fig. 6 that two resonant modes coalesce into the one

inside the areas highlighted by open circles. Such a behavior of resonances close to the EP behavior was observed in different dielectric structures [26,33,34,37,40]. There are ways to approach the true singular points of EPs [52,53] by precise two-parametric tuning of the aspect ratio $R_z/R_\perp$ and the refractive index of spheroid that is challengeable experimentally. However, there is also a way to show EPs by encircling the EP through which resonant eigenmodes are interchanged [16] without approaching the EP point. We encircle the EP points shown as open circles in Fig. 6 by three ways. In the
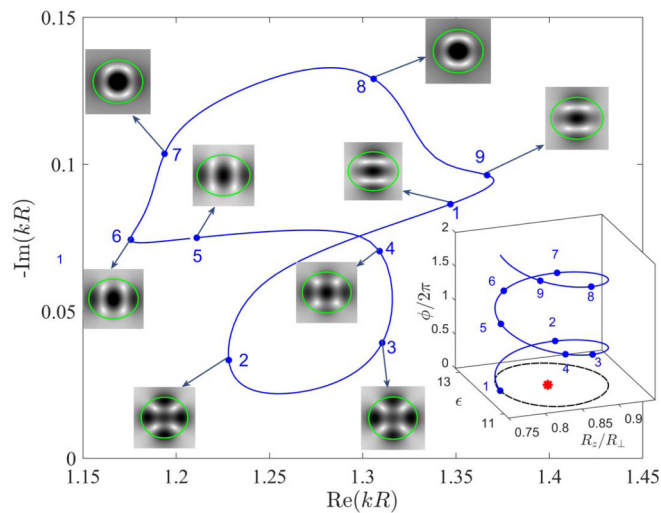

FIG. 8. Evolution of the field patterns E_y for encircling the EP $\epsilon = 12, R_z/R_\perp = 0.84$ marked by star in the sector $m = 1$.
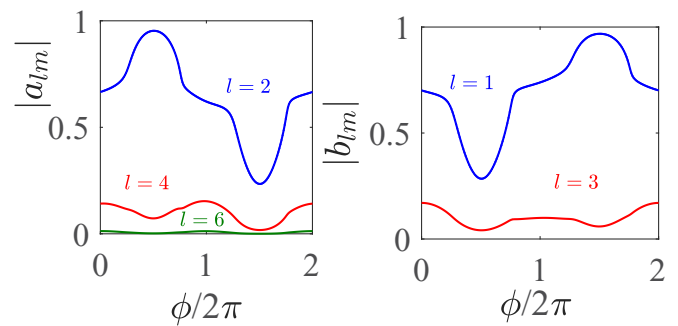

FIG. 9. Evolution of the expansion coefficients a_l^1 (TE modes) and b_l^1 (TM modes) for encircling the EP shown in Fig. 8.

first case the rectangular contour encircles only the left EP at the point $R_z/R_\perp = 0.292$, $\epsilon = 17.2$, as shown in Fig. 7(a). Respectively, in the second case the contour encircles the right EP point $R_z/R_\perp = 0.304$, $\epsilon = 18.4$ as shown in Fig. 7(b). At last, we present also the case of encircling of both EPs shown in Fig. 7(c). In all cases we encircle EPs counterclockwise.

Let us consider the first case shown in Fig. 7(a), where encircling starts with point $R_z/R_\perp = 0.32$, $\epsilon = 17$ marked by an open circle in the inset of the figure. In the first downward path we decrease the aspect ratio at the same permittivity reaching the point till $R_z/R_\perp = 0.27$, $\epsilon = 17$, which is marked by a cross. In the complex plane this path maps into sharp trajectory shown by a dot-dashed blue line that features high response of resonant frequency on the shape of the spheroid. Respectively, the resonant mode demonstrates sharp change of the resonant mode. In the next horizontal path we slightly increase the permittivity from $\epsilon = 17$ to $\epsilon = 17.8$ of the oblate spheroid with the same shape and reach the point $R_z/R_\perp = 0.27$, $\epsilon = 17.8$ marked by a square in the inset. In the complex plane this path maps into monotonic descent of resonant frequency by law $(kR)^2\epsilon \approx C$ or $kR \approx \sqrt{C/17}(1 - \Delta\epsilon/2)$. That linear part of the trajectory is plotted by a solid blue line in Fig. 7(a). The resonant mode presented by the insets at starting and finishing points also does not show visible changes. The third upward part of the rectangular contour goes from the point marked by square $R_z/R_\perp = 0.27$, $\epsilon = 17.8$ to the point marked by star $R_z/R_\perp = 0.32$, $\epsilon = 17.8$ maps into sharp trajectory shown by a blue dashed line. However, the resonant mode is not changing the fact that is related to far distance between the left EP and the path as distinct from the first downward path from circle to cross. By doing so we closed the rectangular contour, however, as the resonant frequency as the resonant mode are interchanged, as was first demonstrated by Dembowskii *et al.* in a microwave metallic resonator [16]. And only the second encircling of the left EP restores the resonant mode as demonstrated in Fig. 7(a) by red lines.

The right EP $R_z/R_\perp = 0.304$, $\epsilon = 18.4$ is expected to give rise to the same features. However, as shown in Fig. 7(b) counterclockwise encircling of this EP demonstrates clockwise behavior of the resonant frequency and mode opposite to the case of counterclockwise encircling of the left EP. That

is related to the fact that the signs of winding numbers of neighboring EPs arising after crossing of two lines in the complex plane are opposite each other [54,55]. Figure 7(c) presents graphical evidence for that. The every encircling of two EPs with opposite winding numbers restores the resonant modes.

Finally, Fig. 8 demonstrates that the EPs are not unique and exist in the sector $m = 1$. Figure 8 demonstrates as for encircling of the EPs in plane $R_\perp/R_z$ and ϵ one of the resonant modes restores only after encircling by 4π in the sector $m = 1$. It is clear that the same refers to the multipole coefficients a_l^1 and b_l^1 as shown in Fig. 9. There are also many other EPs with higher frequencies.

IV. SUMMARY AND CONCLUSIONS

It seems reasonable that resonances of any dielectric particle shaped differently from a sphere yield to the Mie resonances of sphere by the Q factors because the surface of the sphere is minimal. However, as Lai *et al.* [45,46] have shown, that is true only for those resonances whose imaginary part is small enough. We present numerous examples which confirm this rule and give comprehensible insight by demonstration of multipole radiation channels for evolution of a sphere into spheroid. However, we also show exceptions to this rule.

However, the main objective of the present paper was demonstration of EPs in a spheroid that has fundamental significance because of compactness of these dielectric resonators. Moreover, evolution of expansion coefficients in Fig. 4 demonstrates multipole conversion for encircling of EPs and, what is the most remarkable, this evolution has a period 4π. In the photonic system, the appearance of EPs can be exploited to a broad range of interesting applications, including lasing [56], asymmetric mode switching [26], nonreciprocal light transmission [57,58], enhancement of the spontaneous emission [59], and ultrasensitive sensing [60].

ACKNOWLEDGMENT

[1] J. A. Stratton, in *Electromagnetic Theory*, edited by L. A. DuBridge (McGraw-Hill Book Company, Inc., New York, 1941).

[2] P. Conwell, P. Barber, and C. Rushforth, Resonant spectra of dielectric spheres, J. Opt. Soc. Am. A **1**, 62 (1984).

[3] H. M. Lai, P. T. Leung, K. Young, P. W. Barber, and S. C. Hill, Time-independent perturbation for leaking electromagnetic modes in open systems with application to resonances in microdroplets, Phys. Rev. A **41**, 5187 (1990).

[4] E. S. C. Ching, P. T. Leung, A. M. van den Brink, W. M. Suen, S. S. Tong, and K. Young, Quasinormal-mode expansion for waves in open systems, Rev. Mod. Phys. **70**, 1545 (1998).

[5] P. T. Leung, W. M. Suen, C. P. Sun, and K. Young, Waves in open systems via a biorthogonal basis, Phys. Rev. E **57**, 6101 (1998).

[6] J. Okołowicz, M. Płoszajczak, and I. Rotter, Dynamics of quantum systems embedded in a continuum, Phys. Rep. **374**, 271 (2003).

[7] P. Lalanne, W. Yan, K. Vynck, C. Sauvan, and J.-P. Hugonin, Light interaction with photonic and plasmonic resonances, Laser Photonics Rev. **12**, 1700113 (2018).

[8] W. D. Heiss, Repulsion of resonance states and exceptional points, Phys. Rev. E **61**, 929 (2000).

[9] I. Rotter and A. F. Sadreev, Zeros in single-channel transmission through double quantum dots, Phys. Rev. E **71**, 046204 (2005).

[10] J. Wiersig, Formation of Long-Lived, Scarlike Modes Near Avoided Resonance Crossings in Optical Microcavities, Phys. Rev. Lett. **97**, 253901 (2006).

[11] N. R. Bernier, L. D. Tóth, A. K. Feofanov, and T. J. Kippenberg, Level attraction in a microwave optomechanical circuit, Phys. Rev. A **98**, 023841 (2018).

[12] K.-W. Park, S. Moon, H. Jeong, J. Kim, and K. Jeong, Non-hermiticity and conservation of orthogonal relation in dielectric microcavity, J. Phys. Commun. **2**, 075007 (2018).

[13] W. D. Heiss and A. L. Sannino, Avoided level crossing and exceptional points, J. Phys. A: Math. Gen. **23**, 1167 (1990).

[14] W. Heiss, Phases of wave functions and level repulsion, Eur. Phys. J. D **7**, 1 (1999).

[15] H. Eleuch and I. Rotter, Width bifurcation and dynamical phase transitions in open quantum systems, Phys. Rev. E **87**, 052136 (2013).

[16] C. Dembowski, H.-D. Graf, H. L. Harney, A. Heine, W. D. Heiss, H. Rehfeld, and A. Richter, Experimental Observation of the Topological Structure of Exceptional Points, Phys. Rev. Lett. **86**, 787 (2001).

[17] M. Brandstetter, M. Liertzer, C. Deutsch, P. Klang, J. Schöberl, H. E. Türeci, G. Strasser, K. Unterrainer, and S. Rotter, Reversing the pump dependence of a laser at an exceptional point, Nat. Commun. **5**, 4034 (2014).

[18] S. Longhi, Parity-time symmetry meets photonics: A new twist in non-hermitian optics, Europhys. Lett. **120**, 64001 (2017).

[19] L. Feng, R. El-Ganainy, and L. Ge, Non-hermitian photonics based on parity–time symmetry, Nat. Photon. **11**, 752 (2017).

[20] Ş. K. Oezdemir, S. Rotter, F. Nori, and L. Yang, Parity–time symmetry and exceptional points in photonics, Nat. Mater. **18**, 783 (2019).

[21] M.-A. Miri and A. Alù, Exceptional Points in Optics and Photonics, Science **363**, 7709 (2019).

[22] B. Zhen, C. W. Hsu, Y. Igarashi, L. Lu, I. Kaminer, A. Pick, S.-L. Chua, J. Joannopoulos, and M. Soljačić, Spawning rings of exceptional points out of Dirac cones, Nature (London) **525**, 354 (2015).

[23] P. M. Kamiński, A. Taghizadeh, O. Breinbjerg, J. Mørk, and S. Arslanagić, Control of exceptional points in photonic crystal slabs, Opt. Lett. **42**, 2866 (2017).

[24] A. Abdrabou and Y. Y. Lu, Exceptional points of resonant states on a periodic slab, Phys. Rev. A **97**, 063822 (2018).

[25] A. Abdrabou and Y. Y. Lu, Exceptional points of Bloch eigenmodes on a dielectric slab with a periodic array of cylinders, Phys. Scr. **95**, 095507 (2020).

[26] S. N. Ghosh and Y. D. Chong, Exceptional points and asymmetric mode conversion in quasi-guided dual-mode optical waveguides, Sci. Rep. **6**, 19837 (2016).

[27] S. Y. Min, J. Y. Kim, S. Yu, S. G. Menabde, and M. S. Jang, Exceptional Points in Plasmonic Waveguides do not Require Gain or Loss, Phys. Rev. Appl. **14**, 054041 (2020).

[28] L. Feng, X. Zhu, S. Yang, H. Zhu, P. Zhang, X. Yin, Y. Wang, and X. Zhang, Demonstration of a large-scale optical exceptional point structure, Opt. Express **22**, 1760 (2013).

[29] J. Gomis-Bresco, D. Artigas, and L. Torner, Transition from Dirac points to exceptional points in anisotropic waveguides, Phys. Rev. Research **1**, 033010 (2019).

[30] V. Popov, S. Tretyakov, and A. Novitsky, Brewster effect when approaching exceptional points of degeneracy: Epsilon-near-zero behavior, Phys. Rev. B **99**, 045146 (2019).

[31] J.-W. Ryu, S.-Y. Lee, and S. W. Kim, Analysis of multiple exceptional points related to three interacting eigenmodes in a non-Hermitian Hamiltonian, Phys. Rev. A **85**, 042101 (2012).

[32] J. Kullig, C.-H. Yi, M. Hentschel, and J. Wiersig, Exceptional points of third-order in a layered optical microdisk cavity, New J. Phys. **20**, 083016 (2018).

[33] C.-H. Yi, J. Kullig, M. Hentschel, and J. Wiersig, Non-hermitian degeneracies of internal–external mode pairs in dielectric microdisks, Photonics Res. **7**, 464 (2019).

[34] Y. Huang, Y. Shen, and G. Veronis, Non-PT-symmetric two-layer cylindrical waveguide for exceptional-point-enhanced optical devices, Opt. Express **27**, 37494 (2019).

[35] A. Abdrabou and Y. Y. Lu, Exceptional points for resonant states on parallel circular dielectric cylinders, J. Opt. Soc. Am. B **36**, 1659 (2019).

[36] J. Unterhinninghofen, J. Wiersig, and M. Hentschel, Goos-Hänchen shift and localization of optical modes in deformed microcavities, Phys. Rev. E **78**, 016201 (2008).

[37] J. Kullig and J. Wiersig, Perturbation theory for asymmetric deformed microdisk cavities, Phys. Rev. A **94**, 043850 (2016).

[38] J. Kullig, C.-H. Yi, and J. Wiersig, Exceptional points by coupling of modes with different angular momenta in deformed microdisks: A perturbative analysis, Phys. Rev. A **98**, 023851 (2018).

[39] T. Jiang and Y. Xiang, Perturbation model for optical modes in deformed disks, Phys. Rev. A **99**, 023847 (2019).

[40] T. Jiang and Y. Xiang, Perfectly-matched-layer method for optical modes in dielectric cavities, Phys. Rev. A **102**, 053704 (2020).

[41] S. Asano and G. Yamamoto, Light scattering by a spheroidal particle, Appl. Opt. **14**, 29 (1975).

[42] P. Barber and C. Yeh, Scattering of electromagnetic waves by arbitrarily shaped dielectric bodies, Appl. Opt. **14**, 2864 (1975).

[43] S. Hill and R. Benner, Morphology-dependent resonances, in *Optical Effects Associated with Small Particles* (World Scientific, Singapore, 1988), pp. 1–61.

[44] C. Linton, V. Zalipaev, and I. Thompson, Electromagnetic guided waves on linear arrays of spheres, Wave Motion **50**, 29 (2013).

[45] H. M. Lai, C. C. Lam, P. T. Leung, and K. Young, Effect of perturbations on the widths of narrow morphology-dependent resonances in Mie scattering, J. Opt. Soc. Am. B **8**, 1962 (1991).

[46] H. M. Lai, P. T. Leung, and K. Young, Limitations on the photon storage lifetime in electromagnetic resonances of highly transparent microdroplets, Phys. Rev. A **41**, 5199 (1990).

[47] C. C. Lam, P. T. Leung, and K. Young, Explicit asymptotic formulas for the positions, widths, and strengths of resonances in Mie scattering, J. Opt. Soc. Am. B **9**, 1585 (1992).

[48] E. Bulgakov, K. Pichugin, and A. Sadreev, Exceptional points in dielectric spheroid, arXiv:2107.13719v1.

[49] M. V. Rybin, K. L. Koshelev, Z. F. Sadrieva, K. B. Samusev, A. A. Bogdanov, M. F. Limonov, and Y. S. Kivshar, High-Q Supercavity Modes in Subwavelength Dielectric Resonators, Phys. Rev. Lett. **119**, 243901 (2017).

[50] W. Chen, Y. Chen, and W. Liu, Multipolar conversion induced subwavelength high-q kerker supermodes with unidirectional radiations, Laser Photonics Rev. **13**, 1900067 (2019).

[51] E. Bulgakov, K. Pichugin, and A. Sadreev, Mie resonance engineering in two disks, MDPI Photon. **8**, 49 (2021).

[52] R. Uzdin and R. Lefebvre, Finding and pinpointing exceptional points of an open quantum system, J. Phys. B: At., Mol., Opt. Phys. **43**, 235004 (2010).

[53] M. Feldmaier, J. Main, F. Schweiner, H. Cartarius, and G. Wunner, Rydberg systems in parallel electric and magnetic fields: an improved method for finding exceptional points, J. Phys. B: At., Mol., Opt. Phys. **49**, 144002 (2016).

[54] N. Shvartsman and I. Freund, Vortices in Random Wave Fields: Nearest Neighbor Anticorrelations, Phys. Rev. Lett. **72**, 1008 (1994).

[55] K.-F. Berggren, A. F. Sadreev, and A. A. Starikov, Crossover from regular to irregular behavior in current flow through open billiards, Phys. Rev. E **66**, 016218 (2002).

[56] L. Feng, Z. J. Wong, R.-M. Ma, Y. Wang, and X. Zhang, Single-mode laser by parity-time symmetry breaking, Science **346**, 972 (2014).

[57] L. Feng, M. Ayache, J. Huang, Y.-L. Xu, M.-H. Lu, Y.-F. Chen, Y. Fainman, and A. Scherer, Nonreciprocal light propagation in a silicon photonic circuit, Science **333**, 729 (2011).

[58] A. Laha, S. Dey, H. K. Gandhi, A. Biswas, and S. Ghosh, Exceptional point and toward mode-selective optical isolation, ACS Photon. **7**, 967 (2020).

[59] A. Pick, B. Zhen, O. Miller, C. W. Hsu, F. Hernandez, A. Rodriguez, M. Soljačić, and S. Johnson, General theory of spontaneous emission near exceptional points, Opt. Express **25**, 12325 (2017).

[60] W. Chen, Ş. K. Özdemir, G. Zhao, J. Wiersig, and L. Yang, Exceptional points enhance sensing in an optical microcavity, Nature (London) **548**, 192 (2017).